Available online at www.sciencedirect.com
SCIENCE DIRECT®
Journal of Organometallic Chemistry 690 (2005) 2905–2912
Journal of Organometallic Chemistry
www.elsevier.com/locate/jorganchem

# Inclusion of molybdenocene dichloride ($Cp_2MoCl_2$) in 2-hydroxypropyl- and trimethyl-β-cyclodextrin: Structural and biological properties

Susana S. Braga [a], Maria Paula M. Marques [b,c], Joana B. Sousa [b], Martyn Pillinger [a], José J.C. Teixeira-Dias [a], Isabel S. Gonçalves [a,*]

[a] Department of Chemistry, CICECO, University of Aveiro, Campus de Santiago, 3810-193 Aveiro, Portugal
[b] Research Unit "Molecular Physical-Chemistry", University of Coimbra, 3000 Coimbra, Portugal
[c] Biochemistry Department, University of Coimbra, Apt. 3126, 3001-401 Coimbra, Portugal

Received 15 February 2005; revised 9 March 2005; accepted 10 March 2005
Available online 21 April 2005

**Abstract**

Organometallic-cyclodextrin inclusion compounds were obtained by the treatment of molybdenocene dichloride ($Cp_2MoCl_2$) with the modified cyclodextrins (CDs) heptakis-2,3,6-tri-*O*-methyl-β-CD (TRIMEB) and 2-hydroxypropyl-β-CD (HPβCD) in aqueous solution. The products were isolated by liophilisation and characterised in the solid-state by powder XRD, thermogravimetric analysis, Raman and FTIR spectroscopy, and $^{13}C$ CP MAS NMR spectroscopy. The results are consistent with inclusion of $Cp_2MoCl_2$, rather than hydrolysis products such as $[Cp_2Mo(H_2O)X]^+$ (X = Cl, OH) or $[Cp_2Mo(H_2O)_2]^{2+}$. The pure non-included metallocene $Cp_2MoCl_2$ and its inclusion compounds with unmodified β-CD, TRIMEB and HPβCD were screened for their potential antiproliferative and cytotoxic activity, in both human cancer and healthy cell lines. Inclusion in CD was found to enhance the cytotoxic effect of $Cp_2MoCl_2$, with the TRIMEB adduct displaying the highest anti-tumour activity, along with the lowest toxicity towards non-neoplastic cells.


*Keywords:* Cyclodextrins; Molybdenocene; Host–guest chemistry; Cytotoxicity; Human adenocarcinoma

## 1. Introduction

The metallocene dichlorides $Cp_2TiCl_2$, $Cp_2MoCl_2$, $Cp_2VCl_2$ and $Cp_2TiCl_2$ exhibit anti-tumour activity for a wide range of murine and human tumours [1,2]. However, only titanocene dichloride has reached clinical trials so far [3]. These studies have resulted in extensive structure–activity and mechanistic studies on $Cp_2TiCl_2$ in order to understand the mechanism of anti-tumour action [2]. Current evidence is consistent with formation of a Ti(IV) species that lacks the Cp ligands which interacts with DNA, possibly transported into the cell via the iron transporter protein transferrin [4]. Compared with $Cp_2TiCl_2$, $Cp_2MoCl_2$ is an attractive candidate for drug development as the complex is water-soluble and stable to hydrolysis of the Cp ligands at physiological pH [5,6]. On the other hand, $Cp_2MoCl_2$ suffers rapid and extensive hydrolysis of the chloride ligands [5,6a]. $Cp_2MoCl_2$ coordinates to both the nucleobase nitrogens and the phosphate oxygens of nucleotides forming discrete complexes [6a,7]. Recent studies, carried out under physiological conditions, show binding of $Cp_2MoCl_2$ to DNA nitrogen bases, with major affinity for the pur-

* Corresponding author. Tel.: +351 234 378190/370200; fax: +351 234 370084.
*E-mail address:* igoncalves@dq.ua.pt (I.S. Gonçalves).

0022-328X/$ - see front matter © 2005 Elsevier B.V. All rights reserved.
doi:10.1016/j.jorganchem.2005.03.012

ine bases, in particular guanine [8]. Even so, the mechanism of action of $Cp_2MoCl_2$ is still unclear as a previously observed interaction with DNA fragments (calf-thymus) has not been confirmed by recent studies [9]. In fact, interaction with oligonucleotides was only observed at low pH values and absent under physiological conditions [10]. Accordingly, the proposed non-bonded intercalation model with DNA [6a], involving interaction at the phosphate DNA backbone, may not occur. This structure would require a significant helix distortion that may be sterically and energetically unfavourable [9]. Other targets for $Cp_2MoCl_2$ have been sought and interaction with thiol-containing biomolecules was proposed as a relevant biochemical pathway, with serum albumin acting as a plasmic carrier for $Cp_2MoCl_2$ [11]. Concerning intracellular targets, protein kinase C and topoisomerase II were shown to bind $Cp_2MoCl_2$ [12].

Recently, β-cyclodextrin (β-CD) encapsulation of $Cp_2TiCl_2$ [13] and $Cp_2MoCl_2$ [14] was described. CD inclusion compounds are interesting for pharmaceutical use owing to the enhanced solubility, stability and bioavailability of the drug molecules [15,16]. For example, complexation of the promising anti-tumour agent rhodium(II) citrate with hydroxypropyl-β-cyclodextrin (HPβCD) improved encapsulation and release kinetics from biodegradable polymer microspheres [17]. Other potential benefits of using CD drug delivery systems in chemotherapy include improved activities and reduction of toxic side effects. Our preliminary studies indicated that the β-CD · $Cp_2MoCl_2$ inclusion compound exhibits higher chemical stability and a more durable antiproliferative activity [18]. In the present work, we aim to further increase the activity of $Cp_2MoCl_2$ by inclusion in chemically modified cyclodextrin hosts, namely 2,3,6-tri-*O*-methyl-β-CD (TRIMEB) and HPβCD, both of which are much more soluble than the parent β-CD. TRIMEB is widely used in drug delivery as it is superior in protecting the guest from hydrolysis [19]. HPβCD is one of the most popular hosts in the pharmaceutical field, as it greatly increases the guest solubility, acts as an absorption enhancer and, most importantly, features low toxicity [20,21]. In the field of antineoplastic research, HPβCD is often used as a stabiliser, protecting the drug from biodegradation [22]. In association with a porphyrin salt, HPβCD can be used in photodynamic therapy for leukaemia or melanoma [23]. The CD host includes the porphyrin thus protecting its active media from the influence of the biological environment and delivers it intact to the tumoral cells. In the present work, the potential antiproliferative and cytotoxic activities of $Cp_2MoCl_2$ and its inclusion complexes with βCD, HPβCD and TRIMEB were evaluated in the human adenocarcinoma cell line HeLa, and toxicities were also assessed towards healthy cells in human skin fibroblasts.

## 2. Experimental

### 2.1. Materials and methods

Microanalyses and ICP determination of Mo (Eugénio Soares) were performed at the University of Aveiro. Thermogravimetric analysis (TGA) was carried out using a Shimadzu TGA-50 system at a heating rate of 5 K $min^{-1}$ under a static atmosphere of air. Powder XRD data were collected on a Philips X'pert diffractometer using Cu Kα radiation filtered by Ni ($\lambda$ = 1.5418 Å). The IR spectra were recorded on a Unican Mattson Mod 7000 FTIR spectrophotometer using KBr pellets. Raman spectra were recorded on a Bruker RFS 100/S FT-Raman system, using a Nd:YAG laser, 1064 nm excitation (50 mW at the sample position) and a InGaAs detector. Room-temperature solid-state $^{13}C$ CP MAS NMR spectra were recorded at 100.62 MHz on a (9.4 T) Bruker MSL 400P spectrometer, with a 4.5 μs $^1H$ 90° pulse, 2 ms contact time, spinning rate 9 kHz and 12 s recycle delays. Chemical shifts are quoted in parts per million from TMS.

Heptakis-2,3,6-tri-*O*-methyl-β-CD (TRIMEB) was obtained from Fluka and 2-hydroxypropyl-β-CD (HPβCD), with an average degree of substitution of 3, was obtained from Cyclolab, Hungary. $Cp_2MoCl_2$ (**1**) [24] and the inclusion compound βCD · $Cp_2MoCl_2$ (**1c**) [14] were prepared as described previously. Culture media (DMEM-HG), antibiotics (penicillin–streptomycin 100 × solution), cisplatin, EDTA (ethylenediamine-tetraacetic acid, disodium salt, dihydrate), glutamine, Hepes, phenol red (phenolsulfonphthalein), *iso*-propyl alcohol, Trypan blue (0.4% solution, prepared in 0.81% sodium chloride and 0.06% dibasic potassium phosphate), trypsin, trisodium citrate, inorganic salts and acids (of analytical grade) were purchased from Sigma–Aldrich Chemical Co. (Madrid, Spain). Fetal calf serum was obtained from Biochrom KG, Berlin. Alamar blue was acquired from Accurate Chemical & Scientific Corporation, Westbury, NY, USA. The following human cell lines were used: Cervix adenocarcinoma epithelial-like adherent cell line (HeLa), purchased from the European Collection of Cell Cultures (ECACC, UK); Fibroblasts from skin (BJ), obtained from the American Type Culture Collection (ATCC), MD, USA.

### 2.2. TRIMEB · $Cp_2MoCl_2$ (**1a**)

$Cp_2MoCl_2$ (50 mg, 0.17 mmol) was added to a solution of TRIMEB (241 mg, 0.17 mmol) in water (4 ml). The resulting solution was stirred at room temperature for 10 min, then frozen and freeze-dried. The voluminous solid product obtained was rehydrated by exposure to water vapour for 1 h. Anal. found: C, 49.84; H, 7.25; Mo, 4.90. Calc. for $(C_{10}H_{10}Cl_2Mo) \cdot (C_{63}H_{112}O_{35}) \cdot 16\text{-}H_2O$: C, 49.80; H, 6.85; Mo, 4.23%. IR (KBr, $cm^{-1}$):

$\nu$ = 3586m, 3519m, 3099m, 2979s, 2930s, 2895sh, 2831s, 2072w, 1641w, 1460m, 1403w, 1366m, 1321m, 1304m, 1256sh, 1230m, 1195m, 1162vs, 1143vs, 1108vs, 1089vs, 1065vs, 1038vs, 1021sh, 970s, 952m, 910m, 856m, 831m, 808sh, 755m, 705m, 668w, 600sh, 558m, 468w. Raman ($cm^{-1}$): 3124m, 3119m, 3102m, 2977s, 2929s, 2894s, 2829s, 1449m, 1118s, 1061w, 974w, 417w, 414w, 343m, 328vs, 290m, 260w, 211w, 194m, 170sh, 163m, 154m, 129w, 84m. $^{13}C$ CP MAS NMR: $\delta$ = 101.9 (Cp), 100.9, 100.4, 100.1, 99.0, 96.4, 93.9 (TRIMEB, C-1), 88.2, 84.2, 83.5, 82.9, 82.5, 82.0, 81.7, 79.8, 78.0, 77.0, 75.5, 74.4 (TRIMEB, C-2,3,4), 73.2, 72.9, 71.0, 70.6, 69.4 (br, TRIMEB, C-5,6), 63.1, 62.2, 61.7, 61.1, 60.0, 58.7, 58.2, 57.6, 56.0, 55.5 (TRIMEB, O–$CH_3$).

### 2.3. HPβCD · $Cp_2MoCl_2$ (**1b**)

$Cp_2MoCl_2$ (50 mg, 0.17 mmol) was added to a solution of HPβCD (220 mg, 0.17 mmol) in water (4 ml). The resulting solution was stirred at room temperature for 10 min, then frozen and freeze-dried. The voluminous solid product obtained was rehydrated by exposure to water vapour for 1 h. Anal. found: C, 42.03; H, 6.31; Mo, 5.13. Calc. for $(C_{10}H_{10}Cl_2Mo) \cdot (C_{51}H_{88}O_{38}) \cdot 8\text{-}H_2O$: C, 41.86; H, 6.56; Mo, 5.48%. IR (KBr, $cm^{-1}$): $\nu$ = 3379vs, 3118sh, 2968m, 2928s, 2887sh, 1648m, 1460m, 1423m, 1370m, 1335m, 1300m, 1244m, 1156vs, 1123sh, 1082vs, 1033vs, 947s, 850sh, 840m, 818sh, 757m, 705m, 610m, 581m. Raman ($cm^{-1}$): 3367m, 3122s, 2930vs, 2901vs, 1454s, 1382m, 1326s, 1248m, 1117vs, 1079s, 940m, 931m, 839m, 590w, 475w, 411w, 405w, 346sh, 341s, 325vs, 290m, 259w, 206w, 194m, 161m, 154m, 84vs. $^{13}C$ CP MAS NMR: $\delta$ = 102.4 (HPβCD, C-1), 82.2 (HPβCD, C-4), 72.7 (HPβCD, C-2,3,5), 67.0 (host HP group, –O$C_2$CH(OH)$CH_3$), 60.7 (HPβCD, C-6), 19.7 (host HP group, –$OCH_2$CH(OH)$CH_3$).

### 2.4. Cytotoxicity evaluation

#### 2.4.1. Preparation of solutions

All compounds studied were water soluble. Solutions were prepared at concentrations ranging from $2.0 \times 10^{-5}$ to $1.0 \times 10^{-4}$ M in phosphate buffered saline solution (PBS): $132.0 \times 10^{-3}$ M NaCl, $4.0 \times 10^{-3}$ M KCl; $1.2 \times 10^{-3}$ M $NaH_2PO_4$; $1.4 \times 10^{-3}$ M $MgCl_2$; $6.0 \times 10^{-3}$ M glucose; $1.0 \times 10^{-2}$ M Hepes (*N*-[2-hydroxyethyl]piperazine-*N*′-[4-butane-sulfonic acid]). Trypan blue was used as a 0.04% (w/v) solution in PBS.

#### 2.4.2. Cell culture

Stock cultures of cells were maintained at 37 °C, under 5% $CO_2$. HeLa and BJ cells (grown in monolayers) were kept in Dulbecco's modified Eagle's high glucose (4500 mg/l) medium (DMEM-HG), supplemented with 10% heat-inactivated fetal calf serum, glutamine (1.168 g/l) and antibiotics (100 units of penicillin and 100 mg streptomycin). The cell lines were subcultured twice a week. Both HeLa and BJ cells were harvested upon addition of trypsin/EDTA (0.05% trypsin, 0.35 mM EDTA.4Na reconstituted in free $Ca^{2+}$ and $Mg^{2+}$ balanced salt solution).

#### 2.4.3. Toxicity and cell growth inhibition evaluation

Cytotoxicity and cell density evaluation following drug exposure – for drug concentrations of 20–100 μM – were assessed with the use of standard assays. Cells were plated between $2 \times 10^4$ and $3 \times 10^4$ cells/ml on 24-well dishes. Twenty four hours after seeding, drug solutions were added to the medium and the cultures were incubated at 37 °C. Cells were harvested and analysed (both in controls and in drug-treated cultures) every 24 h, for a total period of 3 days. Reversibility of the drug effect was tested by removing the drug and adding fresh culture medium in the last day of incubation with the drug, and assessing the cell viability following four more days of incubation. Cell density and viability were determined by trypan blue exclusion on single-cell suspensions obtained from the monolayer cultures. Cell viability was further assessed through the Alamar blue colorimetric test. All experiments were performed in triplicate.

The Alamar blue assay is a fluorimetric/colorimetric test based on the detection of metabolic activity [25]. It incorporates an oxidation–reduction indicator which changes from the oxidised form – non-fluorescent, blue – to the reduced state – fluorescent, red – in response to chemical reduction of growth medium, as a result of cell growth. For each time point, Alamar blue was added to the cells (both control and drug-treated) and to culture medium (blank), in an amount equal to 10% of the total culture volume. The samples were incubated for 8 h, at 37 °C, and the absorbance was then measured at both 570 nm ($A\lambda_1$, $A'\lambda_1$) and 600 nm ($A\lambda_2$, $A'\lambda_2$) (against the blank). Cell viability is expressed as a percentage of the non-treated control cells and was calculated according to the following equation:

$$\%\text{Reduced} = \frac{(\varepsilon_{OX})\lambda_2 A\lambda_1 - (\varepsilon_{OX})\lambda_1 A\lambda_2}{(\varepsilon_{RED})\lambda_1 A'\lambda_2 - (\varepsilon_{RED})\lambda_2 A'\lambda_1} \times 100, \qquad (1)$$

where $\varepsilon_{OX}$ and $\varepsilon_{RED}$ represent the molar absorptivity coefficients of the oxidised and reduced forms of Alamar blue, respectively, at 570 and 600 nm: $(\varepsilon_{OX})_{\lambda_1} = 80.856$, $(\varepsilon_{RED})_{\lambda_1} = 155.677$, $(\varepsilon_{OX})_{\lambda_2} = 117.216$ and $(\varepsilon_{RED})_{\lambda_2} = 14.652$.

#### 2.4.4. Statistical analysis

All experiments were performed in triplicate and the results are expressed as mean values ± SD (the corresponding error bars being displayed in the graphical plots). Statistical analysis was performed using ANOVA,

followed by post hoc test of Fisher's protected least significant difference. Statistical comparison between the data was based on the Pearson correlation coefficient, values less than 0.05 being considered as significant.

## 3. Results and discussion

### 3.1. Synthesis and characterisation of inclusion compounds

Aqueous solutions of TRIMEB and HPβCD were treated with $Cp_2MoCl_2$ (**1**) and the products TRIMEB · $Cp_2MoCl_2$ (**1a**) and HPβCD · $Cp_2MoCl_2$ (**1b**) isolated by liophilisation. The products were further characterised in the solid-state by powder XRD, TGA, Raman and FTIR spectroscopy, and $^{13}C$ CP MAS NMR. The powder XRD pattern for the TRIMEB adduct **1a** contains a peak at 13.9° 2$\theta$ that indicates the presence of a certain amount of non-included **1** (Fig. 1). However, the overall pattern is significantly different from that simulated for a physical mixture of TRIMEB and **1** in a 1:1 molar ratio. The pattern for **1a** shows some new peaks and the disappearance of others, while a number of the remaining peaks show substantial changes in intensities with some slight changes in the 2$\theta$ values. Nevertheless, the pattern for **1a** contains several peaks that are coincident with peaks exhibited by pure TRIMEB, suggesting that the overall structure of the host was not greatly modified upon interaction with $Cp_2MoCl_2$. Surprisingly, the powder XRD pattern for the experimentally prepared physical mixture is also quite different from the simulated one, and in fact matches well with the pattern for **1a**. It is possible that a weak host–guest interaction occurs even upon mechanical mixing of the two components. These results are different to those obtained for the crystalline 1:1 inclusion complex βCD · $Cp_2MoCl_2$ (**1c**) [14], for which the powder XRD pattern does not contain peaks corresponding either to that of pristine β-CD hydrate or pure non-included **1**. Compound **1b** was poorly crystalline, similar to the pure host HPβCD, and showed only one very broad XRD feature centred around 18° 2$\theta$ (not shown). The amorphous character of these compounds is due to the fact that the modified β-CD is obtained as a mix of CD derivatives with different degrees of substitution, averaging three 2-hydroxypropyl moieties per β-CD molecule.

The thermogravimetric profiles of **1**, TRIMEB, HPβCD, 1:1 physical mixtures of each host with **1**, and the inclusion compounds **1a**–**b** are shown in Figs. 2 and 3. The guest **1** shows one major mass loss of about 60% starting around 170 °C and ending at 330 °C. TRIMEB decomposition occurs in the same temperature range, but features another small step from 350 to 500 °C (Fig. 2). Interestingly, both the physical mixture and TRIMEB · $Cp_2MoCl_2$ (**1a**) present a slightly higher

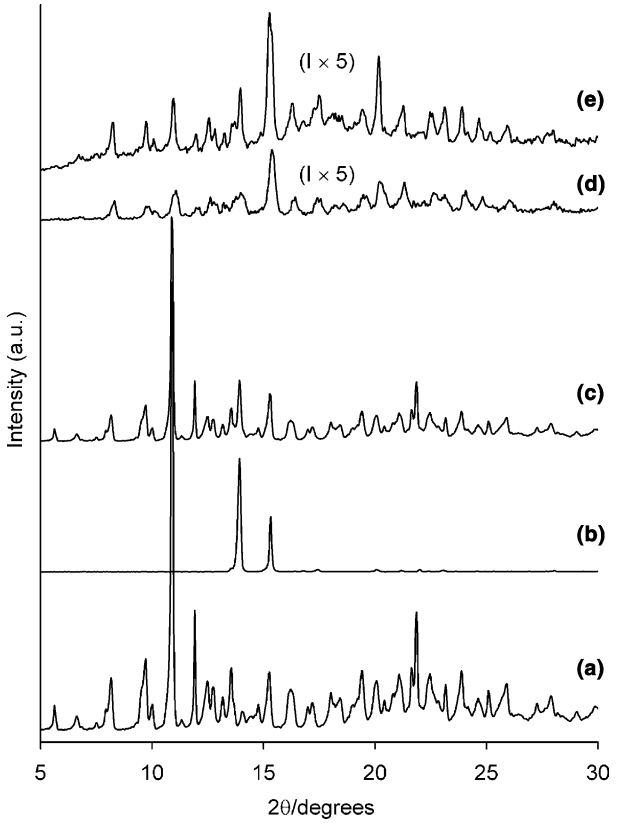


Fig. 1. Powder XRD of: (a) pure TRIMEB; (b) $Cp_2MoCl_2$ (**1**); (c) a simulated physical mixture of TRIMEB and **1** in a 1:1 molar ratio; (d) the experimentally prepared physical mixture of TRIMEB and **1** in a 1:1 molar ratio; and (e) TRIMEB · $Cp_2MoCl_2$ (**1a**).

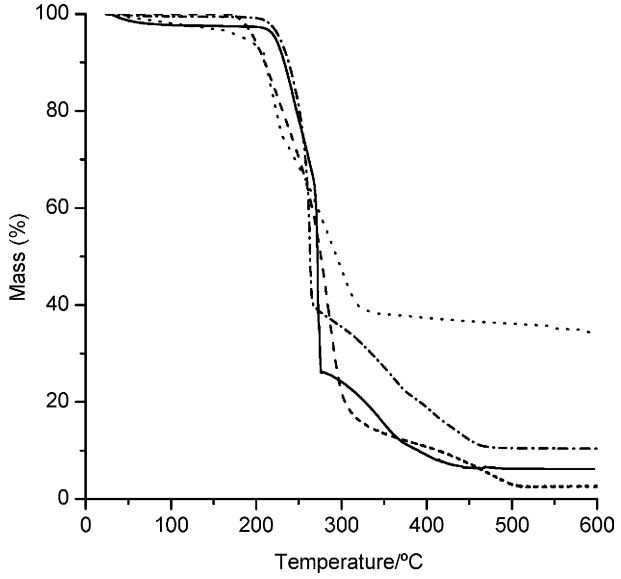


Fig. 2. TGA of TRIMEB · $Cp_2MoCl_2$ (**1a**) (—), pure TRIMEB (– – –), $Cp_2MoCl_2$ (**1**) (· · ·) and a physical mixture of TRIMEB and **1** in a 1:1 molar ratio (–·–·–).

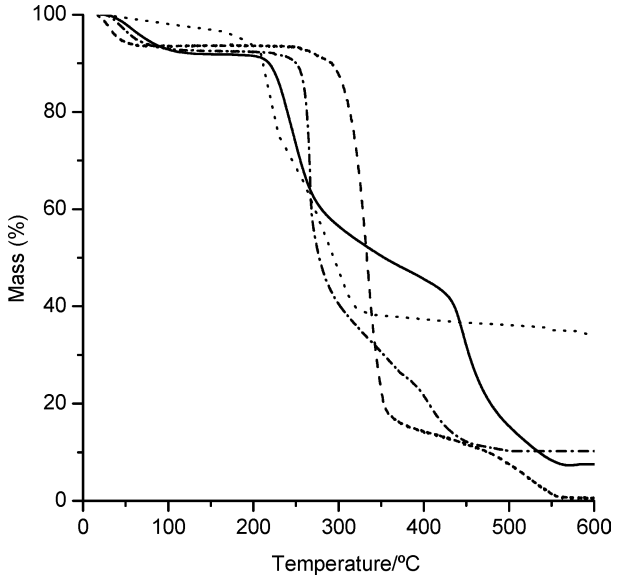


Fig. 3. TGA of HPβCD · $Cp_2MoCl_2$ (**1b**) (—), pure HPβCD (– – –), $Cp_2MoCl_2$ (**1**) (· · ·) and a physical mixture of HPβCD and **1** in a 1:1 molar ratio (–·–·–).

thermal stability, starting to decompose at 200 °C only. This is rather unexpected since the interaction between organometallic guests and cyclodextrins usually results in a lower degradation temperature [14,26]. Still, one may infer that this feature reflects a weak TRIMEB/$Cp_2MoCl_2$ interaction. These considerations are further supported by vibrational spectroscopy data, discussed below.

The HPβCD trace shows loss of hydration water, unlike that of TRIMEB (Fig. 3). Dehydration (6% mass loss) corresponds to a loss of about 4.5 water molecules per HPβCD molecule. At 250 °C the CD decomposition begins, appearing as a very sharp mass loss up to 360 °C. From this point onward, the mass loss is smoother and is complete at 560 °C. The physical mixture features dehydration and starts decomposing at the lower temperature of 230 °C. Compound HPβCD · $Cp_2MoCl_2$ (**1b**), however, starts decomposing at an even lower temperature, around 200 °C. It then exhibits a decomposition trace quite different from that of the mixture, since the first decomposition step ends around 280 °C and is followed by a smoother mass loss up to 425 °C. At this point there is a strong second step that ends at 560 °C and leaves a residual mass of 7.5%. As mentioned above, the earlier onset of thermal decomposition is quite common in organometallic-cyclodextrin inclusion compounds and has been interpreted as the result of a strong host–guest interaction. The TG trace for the physical mixture indicates that some interaction occurs between the two components upon grinding and heating up to 200 °C. The interaction in the inclusion compound **1b** is stronger and therefore the thermal decomposition point is even lower.

Fig. 4 shows the $^{13}C$ CP MAS NMR spectra for $Cp_2MoCl_2$ (**1**), TRIMEB, HPβCD and the inclusion compounds **1a**–**b**. The spectrum of TRIMEB contains several resonances for each type of carbon atom, as observed for the parent β-cyclodextrin [14]. By reference to reported solution spectra [27], the different carbon resonances are assigned to C-1 (93–101 ppm), C-2,3,4 (74–88 ppm), C-5,6 (69–73 ppm) and O–$CH_3$ (55–63 ppm). The spectrum for TRIMEB · $Cp_2MoCl_2$ (**1a**) also shows several resonances for each type of carbon atom, suggesting a weak host–guest interaction, although many of the peaks are shifted and do not coincide with those exhibited by TRIMEB. In addition to the resonances

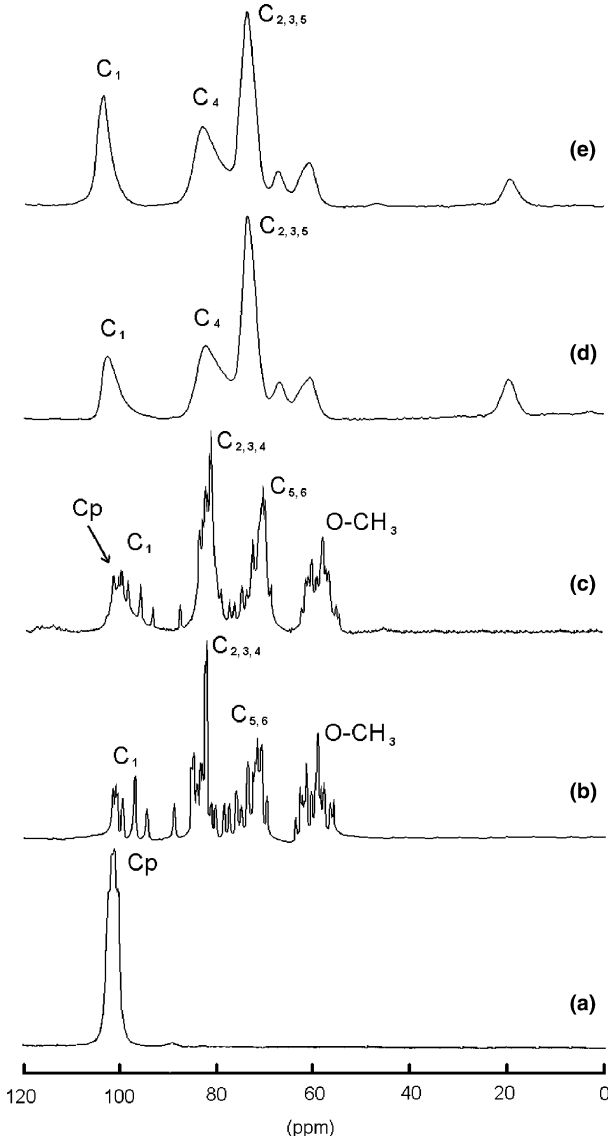


Fig. 4. $^{13}C$ CP MAS NMR spectra of: (a) $Cp_2MoCl_2$ (**1**); (b) TRIMEB, with an approximate description of the carbon resonances; (c) TRIMEB · $Cp_2MoCl_2$ (**1a**); (d) HPβCD, with an approximate description of the carbon resonances; and (e) HPβCD · $Cp_2MoCl_2$ (**1b**).

for the host carbons, the spectrum contains a peak at 101.9 ppm which is assigned to the Cp groups of the guest molecule and is unshifted compared with the resonance for pure non-included **1**. For hydroxypropyl-β-CD and HPβCD · $Cp_2MoCl_2$ (**1b**), only broad lines are observed in the $^{13}C$ CP MAS NMR spectra. The resonance for the cyclopentadienyl carbon atoms is not observed as it overlaps with the broad C-1 host signal.

The KBr IR spectra of compounds **1a** and **1b** do not reveal any measurable changes in the cyclodextrin bands, indicating no chemical modification of the hosts. In addition, some of the vibrational bands due to the guest molecules are observed and the most important ones are listed in Table 1. For compound **1a** these bands are essentially unshifted compared with those for pure non-included $Cp_2MoCl_2$ (**1**), indicating a weak host–guest interaction. In contrast, there are some significant shifts for compound **1b** which point to a stronger host–guest interaction. The Cp *ν*(CH) mode, found at 3100 $cm^{-1}$ for **1**, appears as a weak shoulder at 3118 $cm^{-1}$ in **1b**. Also, the CH out-of-plane bend, featuring two bands at 829 and 807 $cm^{-1}$ for compound **1**, appears shifted, with maxima at 838 and 818 $cm^{-1}$ in compound **1b**. These bands were also found to shift to higher frequency upon encapsulation of **1** in β-CD [14]. Blue-shifts of *ν*(CH) and π(CH) modes in similar metal–cyclopentadienyl complexes have been previously associated with an increase in the covalency of the Cp–M bond [28]. However, more recent vibrational studies discard this hypothesis in favour of an increase in the electron density in the Cp ring [29]. Several low wavenumber bands of **1** are identified in the Raman spectra of **1a** and **1b**, assigned to Mo–Cp and Mo–Cl modes (Table 1). These are essentially unshifted compared with the free non-included organometallic **1**, indicating that $Cp_2MoCl_2$ is the species incorporated in the CD cavities, rather than hydrolysis products such as $[Cp_2Mo(H_2O)X]^+$ (X = Cl, OH) or $[Cp_2Mo(H_2O)_2]^{2+}$.

Table 1
Selected FTIR and Raman data for $Cp_2MoCl_2$ (**1**), TRIMEB · $Cp_2MoCl_2$ (**1a**) and HPβCD · $Cp_2MoCl_2$ (**1b**)

| Observed frequency ($cm^{-1}$) | | | Approximate description |
|---|---|---|---|
| **1** | **1a** | **1b** | |
| *Data from FTIR* | | | |
| 3100 | 3099 | 3118 | Cp C–H stretch |
| 1423 | [a] | 1423 | Cp C⇢C stretch |
| 829, 807 | 831, 808 | 838, 818 | Cp C–H bending, out-of-plane |
| *Data from Raman* | | | |
| 342 | 343 | 341 | Cp–ring tilt |
| 325 | 328 | 325 | Mo–Cp symmetric stretch |
| 288 | 290 | 290 | Mo–Cp asymmetric stretch |
| 264 | 260 | 259 | Mo–Cl symmetric stretch |
| 192, 156 | 194, 154 | 194, 154 | Mo–Cp bending mode |

[a] This band is not visible in compound **1a** due to overlap with TRIMEB bands.

Finally, considering that HPβCD encapsulation strongly affects the cyclopentadienyl C–H vibrations, we may propose that at least one and perhaps both of the Cp ligands are incorporated in the CD cavity. The inclusion geometry associated with the incorporation of both Cp groups would create a steric confinement that could account for the observed shifts of the CH stretching and bending vibrations to higher energy.

### 3.2. Cytotoxicity studies

Growth-inhibition and cytotoxic activities against a human adenocarcinoma (HeLa) and skin non-cancer cells (BJ fibroblasts) were assessed for $Cp_2MoCl_2$ (**1**), TRIMEB · $Cp_2MoCl_2$ (**1a**), HPβCD · $Cp_2MoCl_2$ (**1b**) and βCD · $Cp_2MoCl_2$ (**1c**). For comparison, the clinically used drug cisplatin [*cis*-diaminedichloroplatinum(II)] was also tested. Experiments were carried out using the trypan blue and the Alamar blue colorimetric tests, and the data obtained from both tests were in very good agreement. From the time-response curves – cell density and viability variation as a function of the incubation time with the drug – plotted for the distinct compounds (for concentrations between 20 and 100 μM) and cell lines studied, the chemical characteristics of these compounds were correlated with their anti-tumour activity, and the reversibility and specificity of the growth-inhibition and/or cytotoxic effect were investigated.

Fig. 5 shows the results obtained for HeLa cancer cells and drug concentrations of 50 mM. Inclusion of $Cp_2MoCl_2$ in the CD hosts leads to a higher antiproliferative and cytotoxic effect towards the HeLa cells, after 72 h of incubation. Among the inclusion compounds tested, TRIMEB · $Cp_2MoCl_2$ (**1a**) displayed a slightly more pronounced cytotoxicity towards cancer cells (up to 60% viability decrease, for a 72 h incubation period). Insertion of substituent groups in cyclodextrins affects mainly their solubility and solubilising properties. Full methylation of β-CD makes it highly soluble in both water and most organic solvents and partial hydroxypropylation of β-CD yields a highly water-soluble derivative. These solubility changes influence the in vivo carrier effect of CDs and may thus contribute to the different antiproliferative activities of the inclusion compounds.

A significant disadvantage of the presently used chemotherapeutic agents is their rather high toxicity, mainly due to side reactions with other biomolecules apart from DNA (e.g., proteins). In order to evaluate this factor for the compounds under study, cytotoxicity experiments were carried out in non-neoplastic cells (human fibroblasts from skin). The results obtained led to the conclusion that $Cp_2MoCl_2$ (**1**) and βCD · $Cp_2MoCl_2$ (**1c**) have a rather high toxicity towards these healthy cells, as viability decreases to a minimum of 30%, for a 72 h incubation period (Fig. 6). In contrast, both

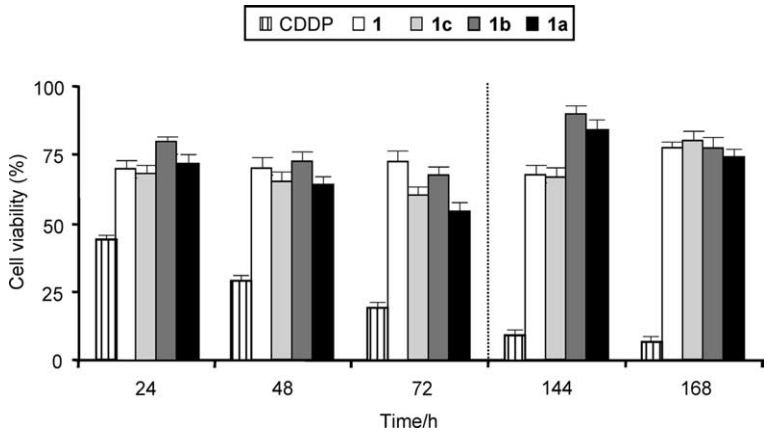


Fig. 5. Time-dependence of the cytotoxic effect of compounds $Cp_2MoCl_2$ (**1**), $\beta CD \cdot Cp_2MoCl_2$ (**1c**), $HP\beta CD \cdot Cp_2MoCl_2$ (**1b**) and $TRIMEB \cdot Cp_2MoCl_2$ (**1a**) (50 mM) towards the HeLa cell line. The cells ($3 \times 105$ cells/ml) were incubated with the drugs for periods of 24–72 h. Every 24 h, aliquots of the cell suspensions were removed and the cell viability was evaluated by the Alamar blue colorimetric assay (as described in Section 2). In addition, the drug was removed 72 h after seeding and the cell viability was assessed following a further incubation of 96 h. The data are expressed as a percentage of the control Alamar reduction (100%) and represent the average ± mean standard deviation from experiments carried out in triplicate. Cisplatin (CDDP) is included for comparison purposes. Intergroup comparison: $p < 0.01$.

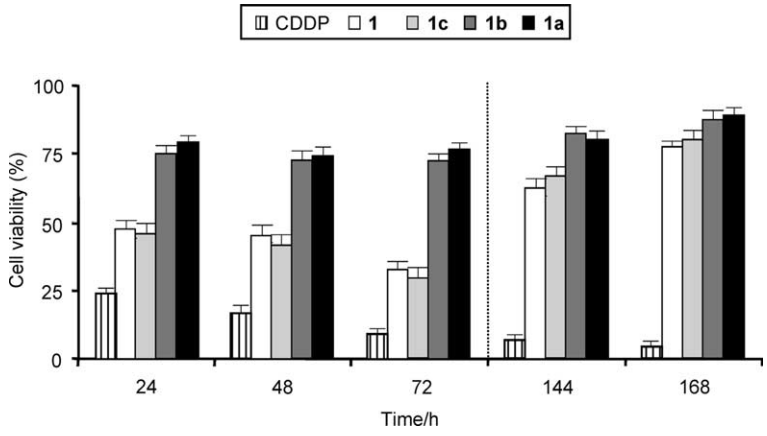


Fig. 6. Time-dependence of the cytotoxic effect of compounds $Cp_2MoCl_2$ (**1**), $\beta CD \cdot Cp_2MoCl_2$ (**1c**), $HP\beta CD \cdot Cp_2MoCl_2$ (**1b**) and $TRIMEB \cdot Cp_2MoCl_2$ (**1a**) (50 mM) towards the BJ cell line. Experimental details are given in the caption to Fig. 5 and also in Section 2.

$TRIMEB \cdot Cp_2MoCl_2$ (**1a**) and $HP\beta CD \cdot Cp_2MoCl_2$ (**1b**) feature a small cell viability decrease with a minimum of ca. 75% for the same incubation period.

The degree of reversibility of both the antiproliferative and cytotoxic effects displayed by compounds aimed for use as antitumour drugs is, understandably, of the utmost importance. In fact, consideration of a recovery period following drug exposure, apart from allowing the determination of the reversibility of the drug effect, as well as the measurement of a possible delayed cytotoxicity, avoids over or underestimation of the level of cell killing achieved. The present results indicate that the antiproliferative and cytotoxic activities of the HPβCD and TRIMEB inclusion compounds are reversible up to 75–80% for the HeLa cells, and up to 85–90% for fibroblasts (96 h after removal of the drug, Fig. 5). Free $Cp_2MoCl_2$ (**1**) and $\beta CD \cdot Cp_2MoCl_2$ (**1c**) display a lower reversibility, both for cancer cells and fibroblasts (Figs. 5 and 6). Moreover, for $TRIMEB \cdot Cp_2MoCl_2$ (**1a**) and $HP\beta CD \cdot Cp_2MoCl_2$ (**1b**), the results reveal an increase in reversibility towards the fibroblasts from 3 to 4 days after drug removal, in contrast to the HeLa cell line. The coupling of high cytotoxicity against cancer lines with low toxicity towards healthy cells is of the utmost relevance for the potential use of these compounds as anticancer agents.

## 4. Conclusions

In this work, organometallic-cyclodextrin inclusion compounds were obtained by the treatment of $Cp_2MoCl_2$ with the modified CDs TRIMEB and HPβCD in aqueous solution. On the basis of the solid-state characterisation data, the incorporated species are tentatively assigned as $Cp_2MoCl_2$, rather than

hydrolysis products such as $[Cp_2Mo(H_2O)X]^+$ (X = Cl, OH) or $[Cp_2Mo(H_2O)_2]^{2+}$. The same conclusion was reached previously for the corresponding β-CD adduct [14]. Furthermore, the results point to a weak host–guest interaction in the TRIMEB adduct, while encapsulation in β-CD and HPβCD features a stronger interaction with possible inclusion geometries involving penetration of one or both Cp ligands into the cyclodextrin cavities. The cytotoxicity experiments carried out on human adenocarcinoma cells indicate that the anti-tumour activity of $Cp_2MoCl_2$ can be enhanced by association with cyclodextrins. The activity increase is coherent with the solubilising and protective effects exerted by cyclodextrins. For the systems studied, TRIMEB · $Cp_2MoCl_2$ was the most effective antiproliferative and cytotoxic agent, exhibiting a 60%, hardly reversible, viability decrease in adenocarcinoma and low toxicity towards healthy cells. This could be associated with a local cell membrane permeability enhancement effect that is higher for methylated cyclodextrins. In fact, comparative studies featuring β-CD, HPβCD and dimethyl-β-CD (DIMEB) showed that DIMEB features a higher absorption-enhancement effect towards skin cells [30]. Further studies will be required in order to validate this possibility.

## Acknowledgements

The authors are grateful to FCT, POCTI and FEDER for financial support (including a postdoctoral grant to S.S.B.). We also thank Paula Esculcas for assistance in measuring the NMR spectra, Celeste Azevedo for the TGA results and Paula Brandão for the powder XRD data.

## References

[1] (a) P. Köpf-Maier, H. Köpf, Drugs Future 11 (1986) 297;
(b) P. Köpf-Maier, T. Klapötke, J. Cancer Res. Clin. Oncol. 118 (1992) 216.
[2] M.M. Harding, G. Mokdsi, Curr. Med. Chem. 7 (2000) 1289.
[3] (a) C.V. Christodoulou, D.R. Ferry, D.W. Fyfe, A. Young, J. Doran, T.M. Sheehan, A. Eliopoulos, K. Hale, J. Baumgart, G. Sass, D.J. Kerr, J. Clin. Oncol. 16 (1998) 2761;
(b) A. Korfel, M.E. Scheulen, H.J. Schmoll, O. Gründel, A. Harstrick, M. Knoche, L.M. Fels, M. Skorzec, F. Bach, J. Baumgart, G. Sass, S. Seeber, E. Thiel, W.E. Berdel, Clin. Cancer Res. 4 (1998) 2701;
(c) G. Lümmen, H. Sperling, H. Luboldt, T. Otto, H. Rübben, Cancer Chemother. Pharmacol. 42 (1998) 415;
(d) N. Kröger, U.R. Kleeberg, K. Mross, L. Edler, D.K. Hossfeld, Onkologie 23 (2000) 60.
[4] (a) H. Sun, H. Li, R.A. Weir, P.J. Sadler, Angew. Chem. Int. Ed. 37 (1998) 1577;
(b) M. Guo, H. Sun, H.J. McArdle, L. Gambling, P.J. Sadler, Biochemistry 39 (2000) 10023.
[5] J.B. Waern, M.M. Harding, J. Organomet. Chem. 689 (2004) 4655.
[6] (a) L.Y. Kuo, M.G. Kanatzidis, M. Sabat, A.L. Tipton, T.J. Marks, J. Am. Chem. Soc. 113 (1991) 9027;
(b) J.H. Toney, T.J. Marks, J. Am. Chem. Soc. 107 (1985) 947.
[7] L.Y. Kuo, M.G. Kanatzidis, T.J. Marks, J. Am. Chem. Soc. 109 (1987) 7207.
[8] V. López-Ramos, C.A. Vega, M. Cádiz, E. Meléndez, J. Electroanal. Chem. 565 (2004) 77.
[9] M.M. Harding, G.J. Harden, L.D. Field, FEBS Lett. 322 (1993) 291.
[10] M.M. Harding, G. Mokdsi, J.P. Mackay, M. Prodigalidad, S.W. Lucas, Inorg. Chem. 37 (1998) 2432.
[11] (a) J.B. Waern, M.M. Harding, Inorg. Chem. 43 (2004) 206;
(b) J.B. Waern, C.T. Dillon, M.M. Harding, J. Med. Chem. 48 (2005) 2093.
[12] (a) G. Mokdsi, M.M. Harding, J. Inorg. Biochem. 83 (2001) 205;
(b) L.Y. Kuo, A.H. Liu, T.J. Marks, in: A. Sigel, H. Sigel (Eds.), Metal Ions in Biological Systems, vol. 33, Marcel Dekker, New York, 1996, pp. 53–85.
[13] I. Turel, A. Demsar, J. Kosmrlj, J. Mol. Recogn. Macromol. Chem. 35 (1999) 595.
[14] S.S. Braga, I.S. Gonçalves, M. Pillinger, P. Ribeiro-Claro, J.J.C. Teixeira-Dias, J. Organomet. Chem. 632 (2001) 11.
[15] T. Loftsson, M.E. Brewster, J. Pharm. Sci. 85 (1996) 1017.
[16] R.A. Rajewski, V.J. Stella, J. Pharm. Sci. 85 (1996) 1142.
[17] R.D. Sinisterra, V.P. Shastri, R. Najjar, R. Langer, J. Pharm. Sci. 88 (1999) 574.
[18] S.S. Braga, Ph.D. Thesis, University of Aveiro, Aveiro (2003).
[19] T. Nagai, H. Ueda, K. Uekama, T. Irie, in: J. Szejtli, T. Osa (Eds.), Comprehensive Supramolecular Chemistry, vol. 3, Pergamon, Oxford, 1996, pp. 441–481.
[20] B. Casu, R. Reggiani, G.G. Gallo, A. Vigevani, Tetrahedron 24 (1968) 803.
[21] T. Irie, K. Uekama, J. Pharm. Sci. 86 (1997) 147.
[22] M. Jumaa, L. Chimilio, S. Chinnaswamy, S. Silchenko, V.J. Stella, J. Pharm. Sci. 93 (2004) 532.
[23] (a) J. Mosinger, M. Deumie, K. Lang, P. Dubat, D.M. Wagnerova, J. Photochem. Photobiol. A 130 (2000) 13;
(b) H. Kolárová, J. Mosinger, R. Lenobel, K. Kejlová, D. Jírová, M. Strnad, Toxicol. in Vitro 17 (2003) 775.
[24] (a) I.S. Gonçalves, E. Herdtweck, C.C. Romão, B. Royo, J. Organomet. Chem. 580 (1998) 169;
(b) M.G.B. Drew, V. Felix, I.S. Gonçalves, F.E. Kühn, A.D. Lopes, C.C. Romão, Polyhedron 17 (1998) 1091.
[25] G.R. Nakayama, M.C. Caton, M.P. Nova, Z. Parandoosh, J. Immunol. Methods 204 (1997) 205.
[26] S.S. Braga, I.S. Gonçalves, A.D. Lopes, M. Pillinger, J. Rocha, C.C. Romão, J.J.C. Teixeira-Dias, J. Chem. Soc., Dalton Trans. (2000) 2964.
[27] (a) J.R. Johnson, N. Shankland, I.H. Sadler, Tetrahedron 41 (1985) 3147;
(b) Y. Inoue, Y. Takahashi, R. Chûjô, Carbohydr. Res. 148 (1986) 109;
(c) Y. Yamamoto, M. Onda, Y. Takahashi, Y. Inoue, R. Chûjô, Carbohydr. Res. 170 (1987) 229.
[28] H.P. Fritz, Adv. Organomet. Chem. 1 (1964) 239.
[29] E. Diana, R. Rossetti, P.L. Stanghellini, S.F.A. Kettle, Inorg. Chem. 36 (1997) 382.
[30] J.Y. Legendre, I. Rault, A. Petit, W. Luijten, I. Demuynck, S. Horvath, Y.M. Ginot, A. Cuine, Eur. J. Pharm. Sci. 3 (1995) 311.